Received: 20 April 2018 | Revised: 10 August 2018 | Accepted: 14 August 2018

DOI: 10.1002/ddr.21464

WILEY DDR

RESEARCH ARTICLE

Synthesis, carbonic anhydrase inhibitory activity and antioxidant activity of some 1,3-oxazine derivatives

Rabia Qamar[1] | Aamer Saeed[1] | Maria Saeed[1] | Zaman Ashraf[2] | Qamar Abbas[3] | Mubashir Hassan[4] | Fernando Albericio[5]

Enabling Technologies		Strategy, Management & Health Policy	
Hit, Lead & Candidate Discovery	Preclinical Research & Development	Clinical Research	Post-Market Research

[1]Department of Chemistry, Quaid-i-Azam University, Islamabad, Pakistan

[2]Department of Chemistry, Allama Iqbal Open University, Islamabad, Pakistan

[3]Department of Physiology, University of Sindh, Jamshoro, Pakistan

[4]Department of Biology, College of Natural Sciences, Kongju National University, Gongju, Republic of Korea

[5]School of Chemistry and Physics, University of KwaZulu-Natal, Durban, South Africa

Correspondence
Aamer Saeed, Department of Chemistry, Quaid-i-Azam University, 45320 Islamabad, Pakistan.
Emails: asaeed@qau.edu.pk; aamersaeed@yahoo.com
and
Zaman Ashraf, Department of Chemistry, Allama Iqbal Open University, Islamabad, Pakistan.
Email: mzchem@yahoo.com

Abstract

A series of 1-(6-methyl-2-substituted phenyl-4-thioxo-4*H*-1,3-oxazin-5-yl)ethanones **(3a-n)** were synthesized by the reaction of benzoyl isothiocyanates with active methylene compound acetylacetone in the presence of triethyl amine in a one-pot process. The structures of the products were elucidated by elemental analyses, FT-IR, ^{1}H NMR, ^{13}C NMR, and mass spectroscopy. These new 1,3-oxazine derivatives were evaluated for their inhibitory activity against carbonic anhydrase II. Results for in vitro assay revealed that compound **3b** having 4-methoxy phenyl moiety was the most potent inhibitor with IC_{50} value of 0.144 ± 0.008 μM. It exhibited higher enzyme inhibitory activity as compared to the standard acetazolamide (IC_{50} = 0.997 ± 0.061 μM). The compounds **3c**, **3h**, and **3n** also displayed superior inhibitory activities compared to the rest of the synthesized oxazine derivatives. The radical scavenging activity of oxazine derivatives was also performed and it was found that compounds showed moderate antioxidant activity. Lipinski rule confirmed the therapeutic potential of the synthesized compounds. Molecular docking studies were also performed to further understand the binding affinity of these compounds with PDBID 1V9E which confirmed that the synthesized derivatives bind in the active binding site of the target protein. Based upon our results, it is proposed that compound **3b** may serve as a lead structure to design more potent carbonic anhydrase inhibitors.

KEYWORDS

1,3-oxazine, acyl isothiocyanates, antioxidant activity, carbonic anhydrase inhibition, molecular docking

1 | INTRODUCTION

Carbonic anhydrase zinc metallo-enzyme catalyzes the reversible hydration of carbon dioxide (CO_2) into a proton (H^+) and bicarbonate (HCO_3^-; Mincione, Scozzafava, & Supuran, 2009; Supuran, 2008; Temperini, Innocenti, Scozzafava, Parkkila, & Supuran, 2009). The biosequestration of CO_2 using carbonic anhydrase in situ encapsulated inside electrospun hollow fibers has been described by Cui et al. (2014). It has widely been documented that carbonic anhydrases contribute in vital physiological processes associated with homeostasis, CO_2/HCO_3^-, electrolyte secretion, tumorigenicity, respiration, calcification, and many other biosynthetic reactions (e.g., gluconeogenesis, lipogenesis, and ureagenesis; Alterio et al., 2006; Ebbesen et al., 2009; Hilvo et al., 2008; Thiry, Dogne, Masereel, & Supuran, 2006). Acetazolamide is a well-known example of clinically recognized CA inhibitor used for the treatment of epilepsy, glaucoma, and altitude sickness (Avvaru et al., 2009). Moreover, it has been revealed that CAIs could be employed as active agents for the cure of hypoxic tumor and obesity (Boztas et al., 2014; Sethi et al., 2014; Simone, Fiore, & Supuran, 2008). However, there is a need to enhance the selectivity and inhibition activity of CA inhibitors. So, the design and synthesis of safe and effective CAIs as useful clinical agents is an active area of research in medicinal

chemistry (Gulçin & Taslimi, 2018; Yiğit et al., 2018). Ren et al. have reported the CO_2 sequestration by immobilized carbonic anhydrase on mesoporous cruciate flower-like metal organic framework (Ren et al., 2018).

Oxazines display useful biological activities and constitute an important class of natural and nonnatural products, making these compounds of special interest (Turgut, Pelit, & Köycü, 2007). Most of them are relevant to the biochemistry of enzymes (Lanni et al., 2007) and cytotoxic drugs (Ouberai et al., 2006). Not only a potential candidate for the synthesis of various types of drug sources (Tomasulo, Sortino, & Raymo, 2005), 1,3-oxazine ring system is also useful for thermal ring closing and photo induced ring opening (Sawant, Mhaske, & Wadekar, 2012). A wide range of biological applications such as anticoagulant, antitubercular, antitumor, antimicrobial, as nonsteroidal PR agonist and as neuroprotective drugs (Beena & Akelesh, 2013; Bhat & Pawar, 2008; Fensome et al., 2005; Narita et al., 2009; Sukhorukov et al., 2014) are known to exhibited by 1,3-oxazine containing heterocycles as this 1,3-oxazine motif is found to be unique and versatile in its bio-active functions (Mayekar et al., 2011).

So far, sulfonamides as CA inhibitors have extensively been reported. We want to report a new class of potent carbonic anhydrase inhibitors, and to the best of our knowledge 1,3-oxazine scaffold was not explored as CA inhibitor. By taking into account the biological significance of 1,3-oxazine derivatives, this is an exciting structure to work with for the development of new chemical entities to combat various diseases. Based on the known facts and possible future applications of CA-II inhibitors in various diseases, the identification of new compounds that suppress the CA activity is the current objective of several research groups. In the present study, we reported the expedient synthesis of a library of 1,3-oxazines and evaluated their inhibition profile against therapeutically relevant carbonic anhydrase II. The antioxidant activity of the synthesized compounds was also evaluated as some of the researchers reported the antioxidant potential of the carbonic anhydrase inhibitors (Aksu et al., 2016; Bulut et al., 2018; Öztaskın, Taslimi, Maraş, Gülcin, & Göksu, 2017; Taslimi et al., 2018). The potent inhibitors were also assessed for binding to CA through molecular docking studies.

2 | MATERIALS AND METHODS

2.1 | Chemistry

All chemicals, reagents, and solvents were of best quality, purchased from Sigma–Aldrich Chemical Co. and Merck (Darmstadt, Germany), and were used without further purification. R_f values were determined using aluminum precoated silica gel plates Kiesel 60 F_{254} from Merck (Darmstadt, Germany). Melting points of the compounds were measured in open capillaries using Stuart melting point apparatus (SMP3) and are uncorrected. The IR spectra were recorded on FTS 3000 MX, Bio-Rad Merlin (Excalibur Model) spectrophotometer as pure compounds. ^{1}H NMR and ^{13}C NMR spectra were run on a Bruker 300 MHz and 75.5 MHz NMR spectrometer in $[CD_3]_2CO$ using TMS as an internal standard. Mass spectra were recorded on Agilent technologies 6890N gas chromatograph and an inert mass selective detector 5973 mass spectrometer and the elemental analyses were conducted using a LECO-183 CHNS analyzer.

2.1.1 | Synthesis of acyl isothiocyanates (2a-n), general procedure

The suitably substituted aromatic acids (2 mmol) in slight excess of thionyl chloride (1.2 equiv.) were heated under reflux for 2 hr to yield corresponding acid chloride derivatives. To these freshly prepared acid chlorides, solution of potassium thiocyanate (2 mmol) in dry acetone was added and then stirred for 1.5 hr at room temperature to afford acyl isothiocyanates that were further used in situ.

2.1.2 | Synthesis of 1-(6-methyl-2-substituted phenyl-4-thioxo-4*H*-1,3-oxazin-5-yl)ethanones (3a-n), general procedure

To a solution of freshly prepared benzoyl isothiocyanate (2 mmol) in dry acetone, acetylacetone (2 mmol), and triethyl amine (2 mL) were added and heated under reflux for 8 hr. The progress of the reaction was monitored by thin layer chromatography, upon reaction completion the reaction mixture was poured onto crushed ice. The precipitated solid was filtered off, washed well with distilled water, dried, and then recrystallized from *n*-hexane: ethyl acetate 4:1 to afford pure products **(3a-n)**.

1-(2-[4-Methylphenyl]-6-methyl-4-thioxo-4*H*-1,3-oxazin-5yl) ethanone (3a)

Off white solid; yield: 83%; R_f: 0.58 (n-hexane: ethyl acetate, 1:1); m.p.: 123–124 °C; IR (pure, cm^{-1}): 2,968, 2,879 (C_{sp^3}-H), 1,672 (C═O), 1,610 (C═N), 1,564, 1,455 (Ar—C═C), 1,303 (C═S); ^{1}H NMR (300 MHz, $[CD_3]_2CO$): δ (ppm) 7.92–7.86 (m, 2H, Ar—H), 7.35–7.31 (m, 2H, Ar—H), 2.57 (s, 3H, $COCH_3$), 2.41 (s, 3H, Ar—CH_3), 2.32 (s, 3H, CH_3); ^{13}C NMR (75.5 MHz, $[CD_3]_2CO$): δ (ppm) 191.0 ($\underline{C}OCH_3$), 189.1 (C═S), 166.7 (C═N), 164.0, 150.3, 144.0, 131.1, 129.7, 128.8, 24.3 ($CO\underline{C}H_3$), 21.1 (Ar—CH_3), 17.2 (CH_3); GC–MS: *m/z* (%) = 259.07 (100) [M^+]; anal. calcd. for $C_{14}H_{13}NO_2S$: C, 64.84; H, 5.05; N, 5.40; S, 12.36; found: C, 64.73; H, 5.09; N, 5.57; S, 12.22.

1-(2-[4-Methoxyphenyl]-6-methyl-4-thioxo-4*H*-1,3-oxazin-5-yl) ethanone (3b)

White crystalline solid; yield: 80%; R_f: 0.50 (*n*-hexane: ethyl acetate, 1:1); m.p.: 110–111°C; IR (pure, cm^{-1}): 2,932, 2,840 (C_{sp^3}-H), 1,660 (C═O), 1,640 (C═N), 1,526, 1,430 (Ar—C═C), 1,305 (C═S), 1,237, 1,050 (C—O); ^{1}H NMR (300 MHz, $[CD_3]_2CO$): δ (ppm) 7.99–7.94 (m, 2H, Ar—H), 7.06–7.00 (m, 2H, Ar—H), 4.10 (s, 3H, OCH_3), 2.46 (s, 3H, $COCH_3$), 2.31 (s, 3H, CH_3); ^{13}C NMR (75.5 MHz, $[CD_3]_2CO$): δ (ppm) 190.9 ($\underline{C}OCH_3$), 186.3 (C═S), 166.0 (C═N), 163.5, 159.2, 155.5, 131.2, 122.5, 113.7, 55.0 (Ar—OCH_3), 23.6 ($CO\underline{C}H_3$), 19.1 (CH_3); GC–MS: *m/z* (%) = 275.06 (100) [M^+]; anal. calcd. for $C_{14}H_{13}NO_3S$: C, 61.07; H, 4.76; N, 5.09; S, 11.65; found: C, 61.22; H, 4.70; N, 5.12; S, 11.53.

1-(2-[2,6-Dimethoxyphenyl]-6-methyl-4-thioxo-4*H*-1,3-oxazin-5yl)ethanone (3c)

Off white solid; yield: 78%; R_f: 0.48 (*n*-hexane: ethyl acetate, 1:1); m.p.: 115–116 °C; IR (pure, cm^{-1}): 2,935, 2,852 (C_{sp^3}-H), 1,645 (C═O), 1,595 (C═N), 1,522, 1,435 (Ar—C═C), 1,302 (C═S), 1,232, 1,045 (C—O); ^{1}H NMR (300 MHz, $[CD_3]_2CO$): δ (ppm) 7.29–7.23 (m, 1H,

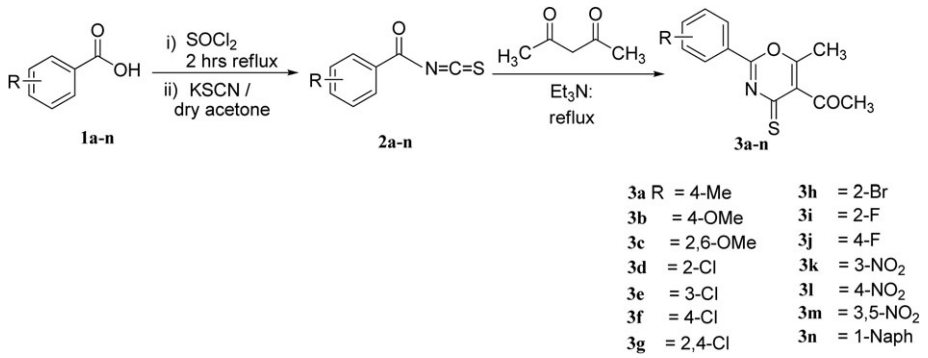

SCHEME 1 Synthetic route to 1-(6-methyl-2-substituted phenyl-4-thioxo-4*H*-1,3-oxazin-5-yl)ethanones **3a-n**

Ar—H), 6.84–6.79 (m, 2H, Ar—H), 3.89 (s, 6H, OCH_3), 2.29 (s, 3H, $COCH_3$), 2.22 (s, 3H, CH_3); ^{13}C NMR (75.5 MHz, $[CD_3]_2CO$): δ (ppm) 194.3 ($\underline{C}OCH_3$), 189.5 (C═S), 164.1 (C═N), 163.4, 162.7, 152.3, 133.1, 128.4, 115.2, 59.2 (Ar—OCH_3), 22.3 ($CO\underline{C}H_3$), 18.7 (CH_3); GC–MS: *m/z* (%) = 305.07 (100) [M^+]; anal. calcd. for $C_{15}H_{15}NO_4S$: C, 59.00; H, 4.95; N, 4.59; S, 10.50; found: C, 59.07; H, 4.67; N, 4.83; S, 10.42.

1-(2-[2-Chlorophenyl]-6-methyl-4-thioxo-4*H*-1,3-oxazin-5-yl) ethanone (3d)

Off white powder; yield: 85%; R_f: 0.55 (*n*-hexane: ethyl acetate, 1:1); m.p.: 184–185 °C; IR (pure, cm^{-1}): 2,931, 2,849 (C_{sp^3}-H), 1,659 (C═O), 1,593 (C═N), 1,530, 1,455 (Ar—C═C), 1,309 (C═S), 778 (C—Cl); ^1H NMR (300 MHz, $[CD_3]_2CO$): δ (ppm) 7.70 (d, 1H, *J* = 6.9 Hz, Ar—H), 7.66 (d, 1H, *J* = 7.3 Hz, Ar—H), 7.59–7.53 (m, 2H, Ar—H), 2.33 (s, 3H, $COCH_3$), 2.21 (s, 3H, CH_3); ^{13}C NMR (75.5 MHz, $[CD_3]_2CO$): δ (ppm) 193.5 ($\underline{C}OCH_3$), 190.5 (C═S), 163.5 (C═N), 162.7, 162.5, 154.7, 134.0, 132.5, 130.6, 129.0, 127.3, 24.1 ($CO\underline{C}H_3$), 17.5 (CH_3); GC–MS: *m/z* (%) = 279.01 (100) [M^+]; anal. calcd. for $C_{13}H_{10}ClNO_2S$: C, 55.82; H, 3.60; N, 5.01; S, 11.46; found: C, 55.88; H, 3.45; N, 5.09; S, 11.62.

1-(2-[3-Chlorophenyl]-6-methyl-4-thioxo-4*H*-1,3-oxazin-5-yl) ethanone (3e)

Off white powder; yield: 83%; R_f: 0.53 (*n*-hexane: ethyl acetate, 1:1); m.p.: 180–181 °C; IR (pure, cm^{-1}): 2,938, 2,845 (C_{sp^3}-H), 1,655 (C═O), 1,597 (C═N), 1,532, 1,454 (Ar—C═C), 1,299 (C═S), 775 (C—Cl); ^1H NMR (300 MHz, $[CD_3]_2CO$): δ (ppm) 7.91–7.87 (m, 1H, Ar—H), 7.82–7.79 (m, 1H, Ar—H), 7.55–7.51 (m, 1H, Ar—H), 7.46–7.40 (m, 1H, Ar—H), 2.25 (s, 3H, $COCH_3$), 2.12 (s, 3H, CH_3); ^{13}C NMR (75.5 MHz, $[CD_3]_2CO$): δ (ppm) 194.2 ($\underline{C}OCH_3$), 187.3 (C═S), 166.5 (C═N), 163.3, 163.7, 135.2, 134.4, 132.4, 131.2, 130.3, 129.5, 23.6 ($CO\underline{C}H_3$), 19.3 (CH_3); GC–MS: *m/z* (%) = 279.01 (100) [M^+]; anal. calcd. for $C_{13}H_{10}ClNO_2S$: C, 55.82; H, 3.60; N, 5.01; S, 11.46; found: C, 55.88; H, 3.45; N, 5.09; S, 11.62.

1-(2-[4-Chlorophenyl]-6-methyl-4-thioxo-4*H*-1,3-oxazin-5-yl) ethanone (3f)

Off white powder; yield: 84%; R_f: 0.52 (*n*-hexane: ethyl acetate, 1:1); m.p.: 186–187 °C; IR (pure, cm^{-1}): 2,945, 2,852 (C_{sp^3}-H), 1,650 (C═O), 1,604 (C═N), 1,548, 1,445 (Ar—C═C), 1,289 (C═S), 772 (C—Cl); ^1H NMR (300 MHz, $[CD_3]_2CO$): δ (ppm) 7.56 (d, 2H, *J* = 7.5 Hz, Ar—H), 7.30 (d, 2H, *J* = 7.5 Hz, Ar—H), 2.25 (s, 3H, $COCH_3$), 2.11 (s, 3H, CH_3); ^{13}C NMR (75.5 MHz, $[CD_3]_2CO$): δ (ppm) 195.0 ($\underline{C}OCH_3$), 188.3 (C═S), 164.2 (C═N), 163.7, 162.4, 136.6, 130.6, 129.0, 128.5, 23.1 ($CO\underline{C}H_3$), 18.0 (CH_3); GC–MS: *m/z* (%) = 279.01 (100) [M^+]; anal. calcd. for $C_{13}H_{10}ClNO_2S$: C, 55.82; H, 3.60; N, 5.01; S, 11.46; found: C, 55.88; H, 3.45; N, 5.09; S, 11.62.

1-(2-[2,4-Dichlorophenyl]-6-methyl-4-thioxo-4*H*-1,3-oxazin-5yl)ethanone (3g)

Brown sticky oil; yield: 55%; R_f: 0.49 (*n*-hexane: ethyl acetate, 1:1); IR (pure, cm^{-1}): 2,948, 2,861 (C_{sp^3}-H), 1,658 (C═O), 1,599 (C═N), 1,554, 1,447 (Ar—C═C), 1,295 (C═S), 780 (C—Cl); ^1H NMR (300 MHz, $[CD_3]_2CO$): δ (ppm) 7.55–7.48 (m, 2H, Ar—H), 7.39 (s, 1H, Ar—H), 2.40 (s, 3H, $COCH_3$), 2.23 (s, 3H, CH_3); ^{13}C NMR (75.5 MHz, $[CD_3]_2CO$): δ (ppm) 194.3 ($\underline{C}OCH_3$), 189.5 (C═S), 165.4 (C═N), 163.0, 163.2, 138.5, 135.4, 132.0, 130.5, 129.7, 127.1, 24.3 ($CO\underline{C}H_3$), 19.5 (CH_3); GC–MS: *m/z* (%) = 312.97 (100) [M^+]; anal. calcd. for $C_{13}H_9Cl_2NO_2S$: C, 49.70; H, 2.89; N, 4.46; S, 10.21; found: C, 49.67; H, 2.94; N, 4.61; S, 10.18.

1-(2-[2-Bromophenyl]-6-methyl-4-thioxo-4*H*-1,3-oxazin-5yl) ethanone (3h)

Light brown powder; yield: 74%; R_f: 0.50 (*n*-hexane: ethyl acetate, 1:1); m.p.: 142–143 °C; IR (pure, cm^{-1}): 2,955, 2,869 (C_{sp^3}-H), 1,669 (C═O), 1,609 (C═N), 1,557, 1,452 (Ar—C═C), 1,280 (C═S), 662 (C—Br); ^1H NMR (300 MHz, $[CD_3]_2CO$): δ (ppm) 7.72 (d, 1H, *J* = 6.3 Hz, Ar—H), 7.58–7.55 (m, 1H, Ar—H), 7.46–7.41 (m, 2H, Ar—H), 2.29 (s, 3H, $COCH_3$), 2.23 (s, 3H, CH_3); ^{13}C NMR (75.5 MHz, $[CD_3]_2CO$): δ (ppm) 193.5 ($\underline{C}OCH_3$), 190.2 (C═S), 165.6 (C═N), 164.3, 163.0, 155.3, 134.5, 133.3, 132.8, 131.5, 127.9, 22.4 ($CO\underline{C}H_3$), 17.4 (CH_3); GC–MS: *m/z* (%) = 324.96 (100) [M^+]; anal. calcd. for $C_{13}H_{10}$ $BrNO_2S$: C, 48.16; H, 3.11; N, 4.32; S, 9.89; found: C, 48.35; H, 3.22; N, 4.39; S, 9.82.

1-(2-[2-Flourophenyl]-6-methyl-4-thioxo-4*H*-1,3-oxazin-5yl) ethanone (3i)

Brown sticky; yield: 53%; R_f: 0.53 (*n*-hexane: ethyl acetate, 1:1); IR (pure, cm^{-1}): 2,962, 2,874 (C_{sp^3}-H), 1,661 (C═O), 1,622 (C═N), 1,560, 1,455 (Ar—C═C), 1,264 (C═S); ^1H NMR (300 MHz, $[CD_3]_2CO$): δ (ppm) 7.81 (d, 1H, *J* = 8.8 Hz, Ar—H), 7.50–7.46 (m, 1H, Ar—H), 7.38

TABLE 1 Carbonic anhydrase II inhibitory activities (IC_{50} in μM) of synthesized 1,3-oxazine derivatives **(3a-n)** and standard acetazolmamide

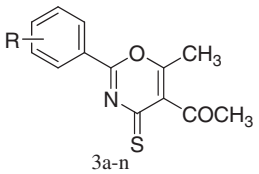

3a-n

Compound	R	$IC_{50} \pm SEM$ (μM)
3a	4-CH_3	1.679 ± 0.099
3b	4-OCH_3	0.144 ± 0.008
3c	2,6-OCH_3	0.328 ± 0.018
3d	2-Cl	2.196 ± 0.125
3e	3-Cl	16.161 ± 0.592
3f	4-Cl	8.235 ± 0.386
3g	2,4-Cl	1.349 ± 0.067
3h	2-Br	0.301 ± 0.012
3i	2-F	3.453 ± 0.214
3j	4-F	27.113 ± 1.612
3k	3-NO_2	32.474 ± 2.134
3l	4-NO_2	2.973 ± 0.175
3m	3,5-NO_2	17.210 ± 1.125
3n	1-Naph	0.317 ± 0.014
Acetazolamide		0.997 ± 0.061

(d, 1H, *J* = 7.3 Hz, Ar—H), 7.29–7.24 (m, 1H, Ar—H), 2.30 (s, 3H, $COCH_3$), 2.19 (s, 3H, CH_3); ^{13}C NMR (75.5 MHz, $[CD_3]_2CO$): δ (ppm) 195.2 ($\underline{C}OCH_3$), 186.4 (C═S), 166.2 (C═N), 163.7, 161.8, 159.7, 132.7, 130.9, 124.5, 118.5, 115.6, 24.2 ($CO\underline{C}H_3$), 19.2 (CH_3); GC–MS: *m/z* (%) = 263.04 (100) [M^+]; anal. calcd. for $C_{13}H_{10}FNO_2S$: C, 59.30; H, 3.83; N, 5.32; S, 12.18; found: C, 59.34; H, 3.79; N, 5.37; S, 12.23.

1-(2-[4-Flourophenyl]-6-methyl-4-thioxo-4*H*-1,3-oxazin-5yl) ethanone (3j)

Light yellow crystalline; yield: 82%; R_f: 0.55 (*n*-hexane: ethyl acetate, 1:1); m.p.: 162–163 °C; IR (pure, cm^{-1}): 2,965, 2,876 (C_{sp^3}-H), 1,663 (C═O), 1,590 (C═N), 1,567, 1,458 (Ar—C═C), 1,264 (C═S); ^{1}H NMR (300 MHz, $[CD_3]_2CO$): δ (ppm) 8.08–8.03 (m, 2H, Ar—H), 7.33–7.27 (m, 2H, Ar—H), 2.72 (s, 3H, $COCH_3$), 2.34 (s, 3H, CH_3); ^{13}C NMR (75.5 MHz, $[CD_3]_2CO$): δ (ppm) 190.4 ($\underline{C}OCH_3$), 185.2 (C═S), 167.0 (C═N), 163.7, 162.8, 153.4, 131.1, 129.9, 115.6, 31.6 ($CO\underline{C}H_3$), 21.4 (CH_3); GC–MS: *m/z* (%) = 263.04 (100) [M^+]; anal. calcd. for $C_{13}H_{10}FNO_2S$: C, 59.30; H, 3.83; N, 5.32; S, 12.18; found: C, 59.34; H, 3.79; N, 5.37; S, 12.23.

1-(2-[3-Nitrophenyl]-6-methyl-4-thioxo-4*H*-1,3-oxazin-5yl) ethanone (3k)

Light yellow solid; yield: 79%; R_f: 0.45 (*n*-hexane: ethyl acetate, 1:1); m.p.: 192–193 °C; IR (pure, cm^{-1}): 2,950, 2,865 (C_{sp^3}-H), 1,662 (C═O), 1,591 (C═N), 1,550, 1,442 (Ar—C═C), 1,547, 1,342 (N═O), 1,292 (C═S); ^{1}H NMR (300 MHz, $[CD_3]_2CO$): δ (ppm) 8.60 (s, 1H, Ar—H), 8.21–8.03 (m, 3H, Ar—H), 2.31 (s, 3H, $COCH_3$), 2.20 (s, 3H, CH_3); ^{13}C NMR (75.5 MHz, $[CD_3]_2CO$): δ (ppm) 195.0 ($\underline{C}OCH_3$), 190.2 (C═S), 166.2 (C═N), 165.0, 162.5, 140.5, 135.7, 132.4, 129.8, 126.3, 124.3, 22.7 ($CO\underline{C}H_3$), 17.3 (CH_3); GC–MS: *m/z* (%) = 290.04 (100) [M^+]; anal. calcd. for $C_{13}H_{10}N_2O_4S$: C, 53.79; H, 3.47; N, 9.65; S, 11.05; found: C, 53.90; H, 3.51; N, 9.33; S, 11.22.

1-(2-[4-Nitrophenyl]-6-methyl-4-thioxo-4*H*-1,3-oxazin-5yl) ethanone (3l)

Off white powder; yield: 81%; R_f: 0.43 (*n*-hexane: Ethyl acetate, 1:1); m.p.: 164–165 °C; IR (pure, cm^{-1}): 2,953, 2,862 (C_{sp^3}-H), 1,665 (C═O), 1,594 (C═N), 1,556, 1,444 (Ar—C═C), 1,542, 1,348 (N═O), 1,310 (C═S); ^{1}H NMR (300 MHz, $[CD_3]_2CO$): δ (ppm) 8.40–8.37 (m, 2H, Ar—H), 8.32–8.25 (m, 2H, Ar—H), 2.56 (s, 3H, $COCH_3$), 2.40 (s, 3H, CH_3); ^{13}C NMR (75.5 MHz, $[CD_3]_2CO$): δ (ppm) 193.5 ($\underline{C}OCH_3$), 186.6 (C═S), 165.1 (C═N), 164.8, 150.6, 148.9, 136.0, 135.5, 130.9, 123.6, 24.3 ($CO\underline{C}H_3$), 18.9 (CH_3); GC–MS: *m/z* (%) = 290.04 (100) [M^+]; anal. calcd. for $C_{13}H_{10}N_2O_4S$: C, 53.79; H, 3.47; N, 9.65; S, 11.05; found: C, 53.90; H, 3.51; N, 9.33; S, 11.22.

1-(2-[3,5-dinitrophenyl]-6-methyl-4-thioxo-4*H*-1,3-oxazin-5yl) ethanone (3m)

Light yellow solid; yield: 87%; R_f: 0.40 (*n*-hexane: ethyl acetate, 1:1); m.p.: 178–179 °C; IR (pure, cm^{-1}): 2,957, 2,865 (C_{sp^3}-H), 1,680 (C═O), 1,601 (C═N), 1,553, 1,448 (Ar—C═C), 1,545, 1,336 (N═O), 1,290 (C═S); ^{1}H NMR (300 MHz, CD_3OD: δ (ppm) 9.21–9.18 (m, 1H, Ar—H), 9.11 (d, 2H, *J* = 3.0 Hz, Ar—H), 2.18 (s, 3H, $COCH_3$), 2.05 (s, 3H, CH_3); ^{13}C NMR (75.5 MHz, CD_3OD: δ (ppm) 194.3 ($\underline{C}OCH_3$), 189.6 (C═S), 166.4 (C═N), 164.5, 163.2, 148.7, 145.4, 133.3, 128.7, 121.9, 25.0 ($CO\underline{C}H_3$), 19.8 (CH_3); GC–MS: *m/z* (%) = 335.02 (100) [M^+]; anal. calcd. for $C_{13}H_9N_3O_6S$: C, 46.57; H, 2.71; N, 12.53; S, 9.56; found: C, 46.69; H, 2.53; N, 12.71; S, 9.80.

TABLE 2 Antioxidant activities (radical scavenging %) of synthesized 1,3-oxazine derivatives **(3a-n)** and standard ascorbic acid

Compound	R	Radical scavenging % (100 μg/mL)
3a	4-CH_3	2.942 ± 0.107
3b	4-OCH_3	28.030 ± 0.691
3c	2,6-OCH_3	1.421 ± 0.0472
3d	2-Cl	8.261 ± 0.285
3e	3-Cl	27.380 ± 0.947
3f	4-Cl	21.194 ± 0.733
3g	2,4-Cl	28.928 ± 1.56
3h	2-Br	0.571 ± 0.097
3i	2-F	36.560 ± 2.265
3j	4-F	12.177 ± 0.621
3k	3-NO_2	1.738 ± 0.040
3l	4-NO_2	0.981 ±0.039
3m	3,5-NO_2	21.635 ±0.986
3n	1-Naph	1.421 ± 0.071
Vitamin C		96.464 ± 2.164

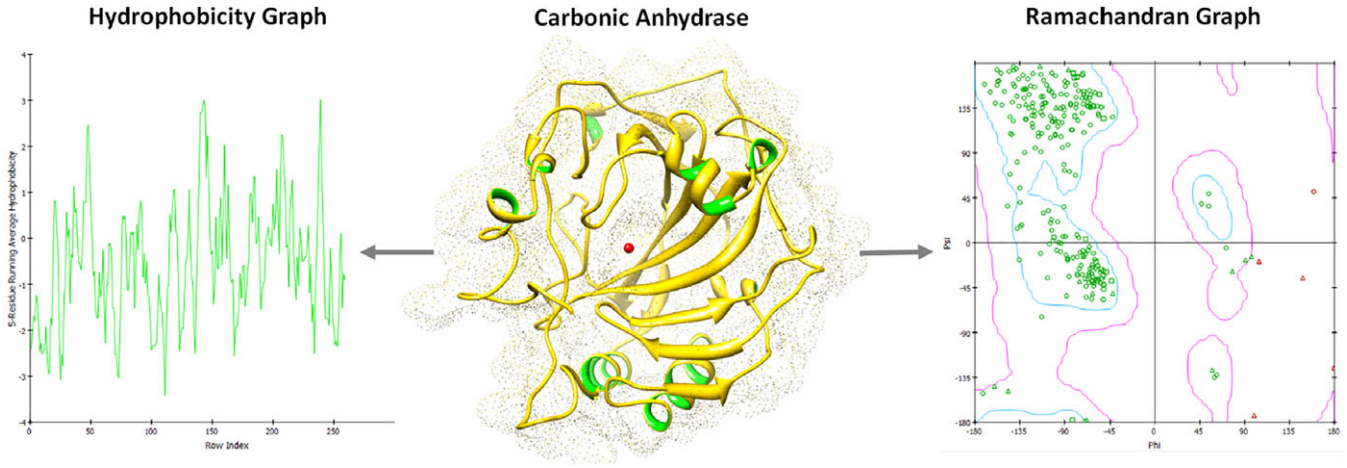

FIGURE 1 Crystal structure of bovine anhydrase II along with hydrophobicity and Ramachandran graphs which shows most of protein residues (93.8%) lies in favored region [Color figure can be viewed at wieyonlinelibrary.com]

1-(2-[1-Naphthoyl]-6-methyl-4-thioxo-4*H*-1,3-oxazin-5yl) ethanone (3n)

Dark brown sticky; yield: 49%; R_f: 0.44 (*n*-hexane: ethyl acetate, 1:1); IR (pure, cm^{-1}): 2,962, 2,874 (C_{sp^3}-H), 1,752 (C═O), 1,602 (C═N), 1,559, 1,463 (Ar—C═C), 1,310 (C═S); ^{1}H NMR (300 MHz, $[CD_3]_2CO$): δ (ppm) 8.39–8.35 (m, 1H, Ar—H), 8.33–8.08 (m, 2H, Ar—H), 7.79–7.60 (m, 1H, Ar—H), 7.93–7.55 (m, 3H, Ar—H), 2.27 (s, 3H, $COCH_3$), 2.20 (s, 3H, CH_3); ^{13}C NMR (75.5 MHz, $(CD_3)_2CO$): δ (ppm) 196.2 ($\underline{C}OCH_3$), 181.3 (C═S), 163.7, 159.4 (C═N), 142.4, 134.2, 133.8, 130.7, 128.3, 127.5, 126.7, 125.9, 29.1 ($CO\underline{C}H_3$), 20.2 (CH_3); GC–MS: *m/z* (%) = 295.07 (100) [M^+]; anal. calcd. for $C_{17}H_{13}NO_2S$: C, 69.13; H, 4.44; N, 4.74; S, 10.86; found: C, 69.20; H, 4.61; N, 4.55; S, 10.79.

2.2 | Carbonic anhydrase assay

Carbonic anhydrase II inhibition was measured as described previously with some modifications (Al-Rashida, Ashraf, Hussain, Nagra, & Abbas, 2011). The method is based on the principle that *p*-nitrophenyl acetate is hydrolyzed by carbonic anhydrase to form yellow colored *p*-nitrophenol which was measured spectrophotometrically. Briefly, reaction mixture contained 120 μL of 50 mM tris–sulfate buffer (pH 7.6 containing 0.1 mM $ZnCl_2$), 20 μL of inhibitor and 20 μL (50 U) bovine enzyme per well. Contents were well mixed and preincubated at 25 °C for 10 min. Substrate *p*-nitrophenyl acetate was prepared (6 mM stock using <5% acetonitrile in buffer and used fresh every time) and 40 μL was added per well to achieve 0.6 mM concentration per well. Total reaction volume was made to 200 μL. After 30 min incubation at 25 °C, contents were mixed and absorbance was measured at 348 nm using a microplate reader. Acetazolamide was used as a reference inhibitor and tris–sulfate buffer was used as negative control. Each concentration was analyzed in three independent experiments. The IC_{50} values were determined by the data analysis and graphing software Origin 8.6, 64-bit. The percent of inhibition of carbonic anhydrase was calculated as following.

TABLE 3 Chemo-informatics properties of synthesized 1,3-oxazine derivatives **(3a-n)**

Ligands	Mol. wt (g/mol)	No. HBA	No. HBD	Mol. Log*P* (mg/L)	PSA (A^2)	Mol. vol (cm^3)	Drug score
3a	259.07	4	0	2.07	31.01	284.25	−1.39
3b	275.06	5	0	1.76	38.56	295.15	−1.43
3c	305.07	6	0	1.61	46.28	327.80	−1.49
3d	279.01	4	0	2.26	31.01	278.63	−0.99
3e	279.01	4	0	2.38	31.01	280.58	−1.33
3f	279.01	4	0	2.38	31.01	280.50	−1.06
3g	312.97	4	0	2.98	31.01	295.90	−0.36
3h	322.96	4	0	2.40	31.01	284.32	−1.35
3i	263.04	4	0	1.82	31.01	268.19	−1.23
3j	263.04	4	0	1.94	31.01	269.22	−1.28
3k	290.04	6	0	1.39	69.28	289.01	−1.12
3l	290.04	6	0	1.39	69.28	288.94	−1.14
3m	335.02	8	0	1.12	107.54	314.80	−1.05
3n	295.07	4	0	3.00	30.74	312.78	−1.43

Abbrevations (HBA = no. of hydrogen bond acceptor; HBD = no. of hydrogen bond donor; Log*P* = lippophilicity of partition coefficient; PSA = polar surface area).

TABLE 4 Docking results of synthesized 1,3-oxazine derivatives **(3a-n)** using glide showing binding affinity with target protein PDBID 1V9E

Docking complexes	Docking score	Glide ligand efficacy	Glide score	Glide energy
3a	−4.22	−0.235	−4.449	−26.45
3b	−4.22	−0.235	−4.449	−26.45
3c	−3.20	−0.153	−3.414	−22.33
3d	−3.47	−0.193	−3.591	−21.61
3e	−3.61	−0.201	−3.804	−25.08
3f	−3.73	−0.207	−3.871	−23.24
3g	−3.54	−0.187	−3.662	−19.87
3h	−2.99	−0.166	−3.152	−18.50
3i	−3.55	−0.198	−3.764	−17.89
3j	−4.49	−0.225	−4.51	−31.89
3k	−4.03	−0.202	−4.055	−25.99
3l	−4.57	−0.229	−4.589	−31.86
3m	−3.69	−0.161	−3.719	−27.96
3n	−3.74	−0.374	−3.956	−23.95

$$\text{Inhibition}\,(\%) = [(B-S)/B] \times 100. \quad (1)$$

Here, the *B* and *S* are the absorbances for the blank and samples.

2.3 | Free radical scavenging assay

Radical scavenging activity was determined by modifying method by 2,2-diphenyl-1-picrylhydrazyl (DPPH) assay (Blois, 1958; Ashraf et al., 2015). The assay solution consisted of 100 μL of (150 μ) 2,2-diphenyl-1 picrylhydrazyl (DPPH), 20 μL of increasing concentration of test compounds and the volume was adjusted to 200 μL in each. This reaction mixture was then incubated for 30 min at room temperature. Ascorbic acid (vitamin C) was used as a reference inhibitor. The measurements were carried out by using a micro plate reader (OPTIMax, tunable) at 517 nm. The reaction rates were compared and the percent inhibition because of the presence of tested inhibitors was calculated. Each concentration was analyzed in three independent experiments.

2.4 | Computational methodology

2.4.1 | Assessment of protein structure from PDB

The three dimensional (3D) crystal structure of carbonic anhydrase II was retrieved form the Protein Data Bank (PDB) having PDBID 1V9E (www.rcsb.org). Energy minimization of target structure was carried out by using conjugate gradient algorithm and Amber force field in UCSF Chimera 1.10.1 (Pettersen et al., 2004). The stereochemical properties, Ramachandran graph and values (Lovell et al., 2003) of carbonic anhydrase II structure were assessed by

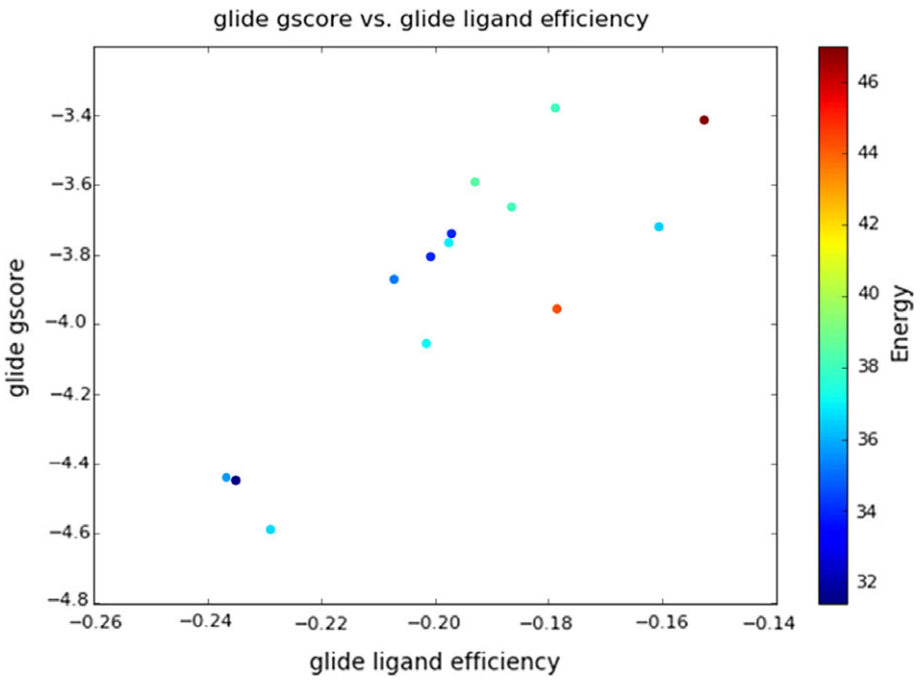

FIGURE 2 Graph depiction between glide energy values and glide score showing ligands efficacy for the target protein PDBID 1V9E [Color figure can be viewed at wieyonlinelibrary.com]

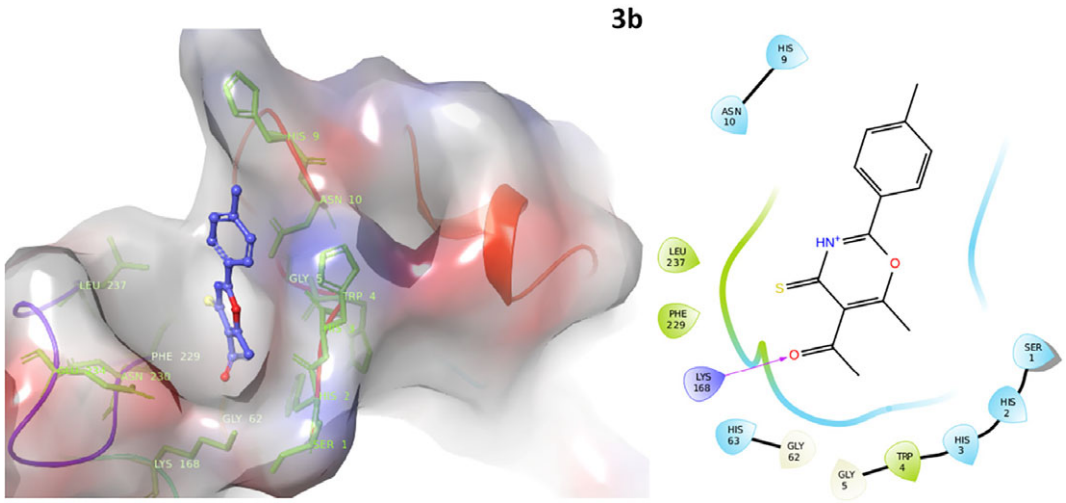

FIGURE 3 Docking interactions of compound **3b** with receptor protein showing carbonyl oxygen of ligand **3b** interacts with Lys168 of target protein, the 2D binding interactions also depicted [Color figure can be viewed at wieyonlinelibrary.com]

Molprobity server (Chen et al., 2010), while the hydrophobicity graph was generated by Discovery Studio 4.1 Client (Studio, 2008). The protein architecture and statistical percentage values of helices, beta-sheets, coils and turns were accessed by using online tool VADAR 1.8 (Willard et al., 2003).

2.4.2 | Ligands preparation

The synthesized compounds **(3a-n)** were sketched in drawing ACD/-ChemSketch tool (http://www.acdlabs.com/products/draw_nom/draw/chemsketch/). The designed ligands were further visualized and minimized by UCSF Chimera 1.10.1. The Molinspiration (http://www.molinspiration.com/) and Molsoft (http://www.molsoft.com/) online computational tools were used to predict the drug-likeness and basic biological properties of these synthesized compounds. Moreover, Lipinski's rule of five was analyzed using Molsoft and Molinspiraion tools. The number of rotatable bonds, H-bond acceptors (HBA), and H-bond donors (HBD) were also confirmed by PubChem (https://pubchem.ncbi.nlm.nih.gov/).

2.4.3 | Grid generation and molecular docking

Prior to molecular docking, the optimized carbonic anhydrase structure was prepared using the "Protein Preparation Wizard" workflow in Schrödinger Suite. Bond orders were assigned and hydrogen atoms were added to the protein. The structure was then minimized to reach the converged root mean square deviation (RMSD) of 0.30 Å with the OPLS_2005 force field. The active site of the enzyme is defined from the co-crystallized ligands from PDB and literature data (Fattah et al., 2018). Furthermore, docking experiment was performed against all synthesized ligands and target protein by using glide docking protocol (Friesner et al., 2006). The predicted binding energies (docking scores) and conformational positions of ligands within active region of protein were also performed using glide experiment. Throughout the docking simulations, both partial flexibility and full flexibility around the active site residues are performed by Glide/SP/XP and induced fit docking (IFD) approaches (Farid, Day, Friesner, & Pearlstein, 2006).

3 | RESULTS AND DISCUSSION

3.1 | Chemistry

The reaction sequence employed for the synthesis of title compounds is shown in Scheme 1. The interaction of equimolar quantities of reactive key substrate benzoyl isothiocyanate **(2a-n)** and methylene active compound acetylacetone in the presence of base triethyl amine gave target products **(3a-n)** in good yields. Acyl isothiocyanates **(2a-n)** were prepared by heating various substituted aromatic acids in slight excess of thionyl chloride. Acyl halides as prepared above gave the corresponding acyl isothiocyanates directly on reaction with metal thiocyanate. The commercially available acetylacetone was employed as carbon nucleophile to react with corresponding aroyl isothiocyanate at its C═N to afford an adduct that underwent subsequent cyclization to yield a variety of desired 1,3-oxazine derivatives in a one-pot process.

^{1}H NMR and ^{13}C NMR data of 1,3-oxazines **(3a-n)** demonstrated in the experimental section is in close agreement with their anticipated structures. ^{1}H NMR revealed the presence of two methyl proton singlets, CH_3 next to the ketone carbonyl appeared at 2.29 ppm while the other CH_3 resonated at a slightly shielded value of 2.22 ppm. ^{13}C NMR displayed three distinct peaks for carbonyl, thiocarbonyl and C═N around 193.2, 190.7 and 165.4 ppm, respectively while the peaks corresponding to two methyl carbons were observed in aliphatic region at δ 23.5 and 19.2. FT-IR spectra exhibited characteristic asymmetric and symmetric stretching absorptions for sp^3C-H at 2,968, 2,879 cm^{-1}. The intense absorption bands for C═N at 1,610 cm^{-1} and for C═O at 1,663 cm^{-1}, in addition to the stretching frequencies of C═C at 1,680 cm^{-1} and C═S around 1,303 cm^{-1} all correspond to oxazine ring structure.

3.2 | Carbonic anhydrase inhibition

The heterocyclic compounds have been synthesized as carbonic anhydrase inhibitors as a different heterocyclic core have been extensively used in the design of more potent carbonic anhydrase inhibitors

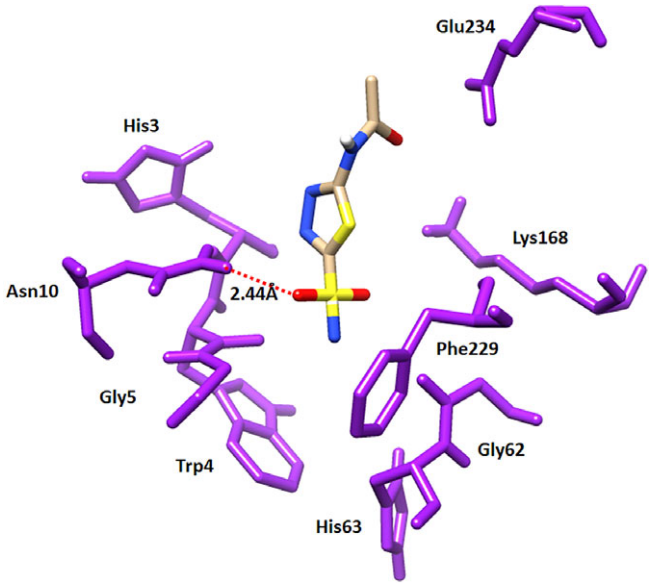

FIGURE 4 Docking interactions of acetazolamide with receptor protein showing sulfonamide oxygen interacts with Asn10 having binding distance 2.44 Å (binding affinity is 6.00 kcal/mol) [Color figure can be viewed at wieyonlinelibrary.com]

(Krasavin et al., 2018). All synthesized compounds **(3a-n)** were tested for their ability to act as carbonic anhydrase II inhibitors. The inhibitory activities of these compounds were examined using standard clinically employed inhibitor acetazolamide. As listed in Table 1, the studied compounds showed different enzyme inhibition profiles. Compound **3b** having 4-methoxy phenyl moiety was the best inhibitor with IC_{50} value 0.144 ± 0.008 μM. Among the series, compounds **3c**, **3h**, and **3n** also proved to be the potent inhibitors of carbonic anhydrase. Halogen on phenyl ring sharply decreased the inhibitory activity of derivatives **3e**, **3f**, and **3j** (16.161, 8.235, 27.113 μM, respectively). While, the analogues with strong electron withdrawing nitro groups that is, **3k** (32.474 ± 2.134 μM) and **3m** (17.210 ± 1.125 μM) also displayed a considerable loss in inhibitory potency.

3.3 | Free radical scavenging

The antioxidant potential of all synthesized compounds **(3a-n)** has been determined using vitamin C as reference to compare the antioxidant activity of the title compounds. Table 2 presented the values obtained from DPPH assay and it was found that the synthesized compounds exhibited low to moderate antioxidant activity. The compound **3b** exhibited 28% radical scavenging activity while **3i** which possess 2-fouloro substitution at phenyl ring showed 36% radical scavenging potential. None of the synthesized compound showed better antioxidant activity than standard ascorbic acid. It is concluded that the synthesized compounds showed good enzyme inhibitory activity compared to antioxidant activity.

3.4 | Structural assessment of carbonic anhydrase II

Carbonic anhydrase II (CA-II) is a zinc containing protein which contains 259 amino acids (Behçet et al., 2018). The structural architecture CA-II showed that it consists of 9% helices, 45% β-sheets, and 45% coils, respectively. The overall the reliability and efficacy of CA-II was confirmed by Ramachandran graph and values. It has been observed that 93.8% of all residues were present in favored regions and only six poor rotamers lies in unfavored regions (Figure 1).

3.5 | Chemo-informatic properties and Lipinski rule (RO5) evaluation of ligands

The synthesized oxazine derivatives were investigated computationally to predict their chemical and bio-molecular properties. The basic prophesied chemoinformatic properties such as molecular weight (MW, g/mol), Log*P*, HBD, HBA, molar volume, polar surface area (PSA), and drug likeness values of all synthesized chemical scaffolds are tabulated in Table 3. Prior research displayed the standard values range for MW and PSA are (160–480 g/mol) and (<89 $Å^2$), respectively (Ghose, Herbertz, Hudkins, Dorsey, & Mallamo, 2012; Kadam & Roy, 2007). The predicted results of synthesized ligands showed that compounds **3a-n** possessed good MW and PSA values which were comparable with standard values. The RO5 analysis also confirmed the therapeutic potential of all the synthesized ligands and all compounds obeyed the RO5 rule. The hydrogen bonding has been recognized as significant parameter for drug permeability. It has been observed that exceeded numbers of HBA (>10) and HBD (>5) results in poor permeation (Bakht, Yar, Abdel-Hamid, Al Qasoumi, & Samad, 2010). Our predicted results showed that all the synthesized ligands possessed <10 HBA and <5 HBD, respectively and their Log*P* values were also comparable with standard value (5). However, multiple examples are available for RO5 violation among the existing drugs (Tian et al., 2015).

3.6 | Docking energy and binding analysis of synthesized compounds

The docked complexes of all oxazines **(3a-n)** against carbonic anhydrase II were analyzed separately and evaluated on the basis of docking score and ligand interactions pattern. Results disclosed that all analogues **(3a-n)** showed good docking scores in the active region of target protein. Docking analysis also justified their good glide ligand efficacy, glide score, and glide energy values as mentioned in Table 4. Although, the basic nucleus of all the synthesized compounds was similar, therefore most of ligands possess good efficient energy values and no big energy difference was observed in all docking complexes. The glide score and ligand efficacy correlation is mentioned in Figure 2.

The ligands–protein binding analyses showed that **3b** is confined in the active binding pocket of target protein as mentioned in Figure 3. The carbonyl group in **3b** interacts with Lys168 and form hydrogen bonding interactions. The other residues which are present around **3b** are Ser1, His2, His3, Trp4, Gly5, His9, Asn10, Gly63, His63, Phe229, and Leu237. Recent literature data also favor our docking results (Fattah et al., 2018). The **3c**-receptor docked complex revealed the good conformational state with good interaction pattern within the receptor binding pocket. The docking result of **3c**-receptor docked complex showed that π–π and hydrophobic bonds were observed at His3 and Lys17 residues, respectively. The residues which are partially involved in surrounding area of ligand are His9, Asn10,

His14, and Asp18. The ligand benzene shows good contact with His3 and form π–π stacking interaction (Supporting Information Figure S2). The 3D and 2D conformations of all docking complexes are mentioned in supplementary data (Supporting Information Figures S1–13).

Acetazolamide docking was performed to check the accuracy of synthetic compounds docking results. Figure 4 showed that Acetazolamide binds against target protein having similar pattern and common residues were seen which binds with drug molecule. A good docking energy value was observed in acetazolamide-carbonic anhydrase docking complex. Some common residues such as His3, Trp4, Gly5, Asn10, Gly62, His63, Lys168, Phe229, and Glu234 were seen around the drug structure. Acetazolamide forms an active hydrogen bond against Asn10 at a distance 2.44 Å. Comparative analyses showed that our designed ligands structure and acetazolamide binding pattern are common in interactions which strengthen our docking results.

4 | CONCLUSIONS

Herein, we reported a simple and straightforward synthesis of 1-(6-methyl-2-substituted phenyl-4-thioxo-4*H*-1,3-oxazin-5-yl)ethanones **(3a-n)** by employing the chemistry of aroyl isothiocyanates. These new compounds possess CA-II inhibition activity and preliminary SAR studies revealed that substituents on phenyl ring play an essential role towards inhibition profile. Docking studies were carried out to predict the binding affinity of synthesized compounds with target protein which assured that most of the synthesized compounds bind at active binding site. It was further analyzed that **3b**-receptor docked complex revealed good interactions with the receptor binding pocket and showed hydrogen bonding interaction with Lys168 residues. Pharmacological investigations confirmed that all ligands possess therapeutic potential so it can be inferred that these new 1,3-oxazine analogues could be further manipulated in drug discovery. Based upon our results it is proposed that compound **3b** may serve as a lead structure to design more potent carbonic anhydrase inhibitors.

ACKNOWLEDGMENTS

We are thankful to Department of Chemistry, Quaid-i-Azam University, Islamabad, Pakistan for providing encouraging environment and facilities for research work.

CONFLICT OF INTEREST

Authors declare no conflict of interest.

ORCID

Aamer Saeed http://orcid.org/0000-0002-7112-9296
Zaman Ashraf http://orcid.org/0000-0002-6620-9080

REFERENCES

Aksu, K., Özgeriş, B., Taslimi, P., Naderi, A., Gülçin, İ., & Göksu, S. (2016). Antioxidant activity, acetylcholinesterase, and carbonic anhydrase inhibitory properties of novel ureas derived from phenethylamines. *Archiv der Pharmazie*, *349*(12), 944–954.

Al-Rashida, M., Ashraf, M., Hussain, B., Nagra, S. A., & Abbas, G. (2011). Discovery of new chromone containing sulfonamides as potent inhibitors of bovine cytosolic carbonic anhydrase. *Bioorganic & Medicinal Chemistry*, *19*, 3367–3371.

Alterio, V., Vitale, R. M., Monti, S. M., Pedone, C., Scozzafava, A., Cecchi, A., … Supuran, C. T. (2006). Carbonic anhydrase inhibitors: X-ray and molecular modeling study for the interaction of a fluorescent antitumor sulfonamide with isozyme II and IX. *Journal of American Chemical Society*, *128*(25), 8329–8335.

Ashraf, Z., Rafiq, M., Seo, S. -Y., Babar, M. M., & Zaidi, N. -U. -S. S. (2015). Design, synthesis and bioevaluation of novel umbelliferone analogues as potential mushroom tyrosinase inhibitors. *Journal of Enzyme Inhibition and Medicinal Chemistry*, *30*, 874–883.

Avvaru, B. S., Busby, S. A., Chalmers, M. J., Griffin, P. R., Venkatakrishnan, B., Agbandje-McKenna, M., … McKenna, R. (2009). Apo-human carbonic anhydrase II revisited: Implications of the loss of a metal in protein structure, stability, and solvent network. *Biochemistry*, *48*(31), 7365–7372.

Bakht, M. A., Yar, M. S., Abdel-Hamid, S. G., Al Qasoumi, S. I., & Samad, A. (2010). Molecular properties prediction, synthesis and antimicrobial activity of some newer oxadiazole derivatives. *European Journal of Medicinal Chemistry*, *45*(12), 5862–5869.

Beena, K., & Akelesh, T. (2013). Design, synthesis, characterization and evaluation of some 1,3-oxazine derivatives as potent antimicrobial agents. *Scholars Research Library*, *5*(4), 257–260.

Behçet, A., Celepci, D. B., Aktaş, A., Taslimi, P., Gök, Y., Aygün, M., & Gülçin, İ. (2018). Synthesis, characterization and crystal structure of 2-(4-hydroxy-phenyl)-ethyl and 2-(4-nitro-phenyl)-ethyl substituted benzimidazole salts: Their inhibitory properties against carbonic anhydrase and acetylcholinesterase. *Journal of Molecular Structure*, *1170*, 160–169.

Bhat, A., & Pawar, P. (2008). Synthesis and biological evaluation of some [1,4]thiazin-2-one and [1,4]oxazin-2-one derivatives. *Indian Drugs*, *45*(12), 962–965.

Blois, M. S. (1958). Antioxidant determinations by the use of a stable free radical. *Nature*, *181*(4617), 1199–1200.

Boztas, M., Cetinkaya, Y., Topal, M., Gülçin, I. l., Menzek, A., Sahin, E., … Supuran, C. T. (2014). Synthesis and carbonic anhydrase isoenzymes I, II, IX, and XII inhibitory effects of dimethoxybromophenol derivatives incorporating cyclopropane moieties. *Journal of Medicinal Chemistry*, *58*(2), 640–650.

Bulut, N., Kocyigit, U. M., Gecibesler, I. H., Dastan, T., Karci, H., Taslimi, P., & Cetin, A. (2018). Synthesis of some novel pyridine compounds containing bis-1,2,4-triazole/thiosemicarbazide moiety and investigation of their antioxidant properties, carbonic anhydrase, and acetylcholinesterase enzymes inhibition profiles. *Journal of Biochemical and Molecular Toxicology*, *32*(1), e22006.

Chen, V. B., Arendall, W. B., Headd, J. J., Keedy, D. A., Immormino, R. M., Kapral, G. J., … Richardson, D. C. (2010). MolProbity: All-atom structure validation for macromolecular crystallography. *Acta Crystallographica Section D: Biological Crystallography*, *66*(1), 12–21.

Cui, J., Li, Y., Ji, X., Bian, H., Zhang, Y., Su, Z., … Zhang, S. (2014). Bio-sequestration of CO_2 using carbonic anhydrase in situ encapsulated inside electrospun hollow fibers. *Chemical Journal of Chinese Universities*, *35*, 1999–2006.

Ebbesen, P., Pettersen, E. O., Gorr, T. A., Jobst, G., Williams, K., Kieninger, J., … Lambin, P. (2009). Taking advantage of tumor cell adaptations to hypoxia for developing new tumor markers and treatment strategies. *Journal of Enzyme Inhibition and Medicinal Chemistry*, *24*-(Suppl 1), 1–39.

Farid, R., Day, T., Friesner, R. A., & Pearlstein, R. A. (2006). New insights about HERG blockade obtained from protein modeling, potential energy mapping, and docking studies. *Bioorganic & Medicinal Chemistry*, *14*(9), 3160–3173.

Fattah, T. A., Saeed, A., Channar, P. A., Larik, F. A., Hassan, M., Raza, H., … Seo, S. -Y. (2018). Synthesis and molecular docking studies of (*E*)-4--(substituted-benzylideneamino)-2*H*-chromen-2-one derivatives: Entry to new carbonic anhydrase class of inhibitors. *Drug Research*, *68*, 378–386. https://doi.org/10.1055/s-0043-123998

Fensome, A., Bender, R., Chopra, R., Cohen, J., Collins, M. A., Hudak, V., … Svenson, K. (2005). Synthesis and structure-activity relationship of

novel 6-aryl-1,4-dihydrobenzo[d][1,3]oxazine-2-thiones as progesterone receptor modulators leading to the potent and selective nonsteroidal progesterone receptor agonist tanaproget. *Journal of Medicinal Chemistry*, *48*(16), 5092–5095.

Friesner, R. A., Murphy, R. B., Repasky, M. P., Frye, L. L., Greenwood, J. R., Halgren, T. A., … Mainz, D. T. (2006). Extra precision glide: Docking and scoring incorporating a model of hydrophobic enclosure for protein–ligand complexes. *Journal of Medicinal Chemistry*, *49*(21), 6177–6196.

Ghose, A. K., Herbertz, T., Hudkins, R. L., Dorsey, B. D., & Mallamo, J. P. (2012). Knowledge-based, central nervous system (CNS) lead selection and lead optimization for CNS drug discovery. *ACS Chemical Neuroscience*, *3*(1), 50–68.

Gulçin, İ., & Taslimi, P. (2018). Sulfonamide inhibitors: A patent review 2013–present. *Expert Opinion on Therapeutic Patents*, *28*(7), 541–549.

Hilvo, M., Salzano, A. M., Innocenti, A., Kulomaa, M. S., Scozzafava, A., Scaloni, A., … Supuran, C. T. (2008). Cloning, expression, post-translational modifications and inhibition studies on the latest mammalian carbonic anhydrase isoform, CA XV. *Journal of Medicinal Chemistry*, *52*(3), 646–654.

Kadam, R., & Roy, N. (2007). Recent trends in drug-likeness prediction: A comprehensive review of in silico methods. *Indian Journal of Pharmaceutical Sciences*, *69*(5), 609–615.

Krasavin, M., Shetnev, A., Sharonova, T., Baykov, S., Tuccinardi, T., Kalinin, S., … Supuran, C. T. (2018). Heterocyclic periphery in the design of carbonic anhydrase inhibitors: 1,2,4-Oxadiazol-5-yl benzenesulfonamides as potent and selective inhibitors of cytosolic hCA II and membrane-bound hCA IX isoforms. *Bioorganic Chemistry*, *76*, 88–97.

Lanni, T. B., Greene, K. L., Kolz, C. N., Para, K. S., Visnick, M., Mobley, J. L., … Liimatta, M. B. (2007). Design and synthesis of phenethyl benzo[1,4]oxazine-3-ones as potent inhibitors of PI3Kinaseγ. *Bioorganic & Medicinal Chemistry Letters*, *17*(3), 756–760.

Lovell, S. C., Davis, I. W., Arendall, W. B., De Bakker, P. I., Word, J. M., Prisant, M. G., … Richardson, D. C. (2003). Structure validation by Cα geometry: φ, ψ and Cβ deviation. *Proteins: Structure, Function, and Bioinformatics*, *50*(3), 437–450.

Mayekar, A. N., Yathirajan, H. S., Narayana, B., Sarojini, B. K., Kumari, N. S., & Harrison, W. T. (2011). Synthesis and antimicrobial study of new 8-bromo-1,3-diaryl-2,3-dihydro-1*H*-naphtho[1,2e][1,3]oxazines. *International Journal of Chemistry*, *3*(1), 74–86.

Mincione, F., Scozzafava, A., & Supuran, C. T. (2009). *Antiglaucoma carbonic anhydrase inhibitors as ophthalomologic drugs*. Hoboken, NJ: Wiley.

Narita, T., Suga, A., Kobayashi, M., Hashimoto, K., Sakagami, H., Motohashi, N., … Wakabayashi, H. (2009). Tumor-specific cytotoxicity and type of cell death induced by benzo[b]cyclohept[e][1,4]oxazine and 2-aminotropone derivatives. *Anticancer Research*, *29*(4), 1123–1130.

Ouberai, M., Asche, C., Carrez, D., Croisy, A., Dumy, P., & Demeunynck, M. (2006). 3,4-Dihydro-1*H*-[1,3]oxazino[4,5-c]acridines as a new family of cytotoxic drugs. *Bioorganic & Medicinal Chemistry Letters*, *16*(17), 4641–4643.

Öztaskın, N., Taslimi, P., Maraş, A., Gülcin, İ., & Göksu, S. (2017). Novel antioxidant bromophenols with acetylcholinesterase, butyrylcholinesterase and carbonic anhydrase inhibitory actions. *Bioorganic Chemistry*, *74*, 104–114.

Pettersen, E. F., Goddard, T. D., Huang, C. C., Couch, G. S., Greenblatt, D. M., Meng, E. C., & Ferrin, T. E. (2004). UCSF chimera—A visualization system for exploratory research and analysis. *Journal of Computational Chemistry*, *25*(13), 1605–1612.

Ren, S., Feng, Y., Wen, H., Li, C., Cui, J., & Jia, S. (2018). Immobilized carbonic anhydrase on mesoporous cruciate flower-like metal organic framework for promoting CO_2 sequestration. *International Journal of Biological Macromolecules*, *117*, 189–198.

Sawant, R. L., Mhaske, M. S., & Wadekar, J. B. (2012). Anticoagulant potential of schiff bases of 1,3-oxazines. *International Journal of Pharmacy and Pharmaceutical Sciences*, *4*(4), 320–323.

Sethi, K. K., Verma, S. M., Tanç, M., Purper, G., Calafato, G., Carta, F., & Supuran, C. T. (2014). Carbonic anhydrase inhibitors: Synthesis and inhibition of the human carbonic anhydrase isoforms I, II, IX and XII with benzene sulfonamides incorporating 4- and 3-nitrophthalimide moieties. *Bioorganic & Medicinal Chemistry*, *22*(5), 1586–1595.

Simone, G. D., Fiore, A. D., & Supuran, C. T. (2008). Are carbonic anhydrase inhibitors suitable for obtaining antiobesity drugs? *Current Pharmaceutical Design*, *14*(7), 655–660.

Studio, D. (2008). *Discovery*, *version 2.1*. San Diego, CA: Accelrys.

Sukhorukov, A. Y., Nirvanappa, A. C., Swamy, J., Ioffe, S. L., Swamy, S. N., & Rangappa, K. S. (2014). Synthesis and characterization of novel 1,2-oxazine based small molecules that targets acetylcholinesterase. *Bioorganic & Medicinal Chemistry Letters*, *24*(15), 3618–3621.

Supuran, C. T. (2008). Carbonic anhydrases: Novel therapeutic applications for inhibitors and activators. *Nature Reviews Drug Discovery*, *7*(2), 168–181.

Taslimi, P., Sujayev, A., Turkan, F., Garibov, E., Huyut, Z., Farzaliyev, V., & Gulçin, İ. (2018). Synthesis and investigation of the conversion reactions of pyrimidine-thiones with nucleophilic reagent and evaluation of their acetylcholinesterase, carbonic anhydrase inhibition, and antioxidant activities. *Journal of Biochemical and Molecular Toxicology*, *32*(2), e22019.

Temperini, C., Innocenti, A., Scozzafava, A., Parkkila, S., & Supuran, C. T. (2009). The coumarin-binding site in carbonic anhydrase accommodates structurally diverse inhibitors: The antiepileptic lacosamide as an example and lead molecule for novel classes of carbonic anhydrase inhibitors. *Journal of Medicinal Chemistry*, *53*(2), 850–854.

Thiry, A., Dogne, J. -M., Masereel, B., & Supuran, C. T. (2006). Targeting tumor-associated carbonic anhydrase IX in cancer therapy. *Trends in Pharmacological Sciences*, *27*(11), 566–573.

Tian, S., Wang, J., Li, Y., Li, D., Xu, L., & Hou, T. (2015). The application of in silico drug-likeness predictions in pharmaceutical research. *Advanced Drug Delivery Reviews*, *86*, 2–10.

Tomasulo, M., Sortino, S., & Raymo, F. M. (2005). A fast and stable photochromic switch based on the opening and closing of an oxazine ring. *Organic Letters*, *7*(6), 1109–1112.

Turgut, Z., Pelit, E., & Köycü, A. (2007). Synthesis of new 1,3-disubstituted-2,3-dihydro-1*H*-naphth [1,2e][1,3]oxazines. *Molecules*, *12*(3), 345–352.

Willard, L., Ranjan, A., Zhang, H., Monzavi, H., Boyko, R. F., Sykes, B. D., & Wishart, D. S. (2003). VADAR: A web server for quantitative evaluation of protein structure quality. *Nucleic Acids Research*, *31*(13), 3316–3319.

Yiğit, B., Yiğit, M., Barut Celepci, D., Gök, Y., Aktaş, A., Aygün, M., & Gülçin, İ. (2018). Novel benzylic substituted imidazolinium, tetrahydropyrimidinium and tetrahydrodiazepinium salts: Potent carbonic anhydrase and acetylcholinesterase inhibitors. *ChemistrySelect*, *3*(27), 7976–7982.

SUPPORTING INFORMATION

Additional supporting information may be found online in the Supporting Information section at the end of the article.

How to cite this article: Qamar R, Saeed A, Saeed M, et al. Synthesis, carbonic anhydrase inhibitory activity and antioxidant activity of some 1,3-oxazine derivatives. *Drug Dev Res*. 2018;1–10. https://doi.org/10.1002/ddr.21464